

Supporting Information

**Exclusive Neural Network Representation of the
Quasi-diabatic Hamiltonians Including Conical
Intersections**

Yingyue Hong,^{†,‡,§} Zhengxi Yin,^{†,‡,§} Yafu Guan,^{†,¶} Zhaojun Zhang,[†] Bina Fu,^{*,†}
and Dong H. Zhang^{*,†}

*State Key Laboratory of Molecular Reaction Dynamics and Center for Theoretical and
Computational Chemistry, Dalian Institute of Chemical Physics, Chinese Academy of Sciences,
Dalian, P.R. China 116023, University of Chinese Academy of Sciences, Beijing 100049, People's
Republic of China, and Department of Chemistry, Johns Hopkins University, Baltimore,
Maryland 21218, USA*

E-mail: bina@dicp.ac.cn; zhangdh@dicp.ac.cn

^{*}To whom correspondence should be addressed

[†]State Key Laboratory of Molecular Reaction Dynamics and Center for Theoretical and Computational Chemistry, Dalian Institute of Chemical Physics, Chinese Academy of Sciences, Dalian, P.R. China 116023

[‡]University of Chinese Academy of Sciences, Beijing 100049, People's Republic of China

[¶]Department of Chemistry, Johns Hopkins University, Baltimore, Maryland 21218, USA

[§]Contributed equally to this work

The FI-NN approach

Since the fitting and interpolation are essentially impossible to reproduce the cuspidal behaviors of adiabatic energies near the conical intersections in the adiabatic representation regardless of the fitting accuracy,¹⁻⁴ the transformation from fitted adiabatic PESs to the diabatic representation would introduce discontinuities and oscillations and thereby substantially diminish the accuracy of diabaticization. Nevertheless, the elements of the diabatic potential energy matrix are smooth functions of nuclear coordinates. Therefore, it is appropriate to represent them with feed-forward NN functions.

The ground and first excited states of NH_3 belong to the A'_1 and A''_2 irreducible representations of the CNPI group, which is the direct product of the symmetry group of order 3 and the inversion group. As discussed previously,⁵ the individual blocks of \mathbf{H}^d , \mathbf{H}_{11}^d , \mathbf{H}_{22}^d and \mathbf{H}_{12}^d , carry A'_1 , A'_1 and A''_2 , respectively, so that the \mathbf{H}_{12}^d term should be antisymmetric with the exchange of two H atoms, while the two diagonal blocks are invariant with respect to the inversion of all nuclei and electrons and permutations of three hydrogen nuclei.

The fundamental invariants (FIs) can be used to account for the permutation invariant symmetry of the two diagonal blocks.^{6,7} The FIs contains the least number of invariants which can generate all the invariant polynomials, and are used as inputs of NNs. For NH_3 , the N atom is denoted as atom 1 and three H atoms are denoted as atoms 2, 3 and 4. The pairwise internuclear distances $r_{12}, r_{13}, r_{14}, r_{23}, r_{24}$ and r_{34} are denoted as $r_i (i = 1, 2, \dots, 6)$, respectively. As follows, there are in

total nine FIs with a maximum degree of three:

$$\begin{aligned}
f_1 &= r_4 + r_5 + r_6 \\
f_2 &= r_1 + r_2 + r_3 \\
f_3 &= r_4^2 + r_5^2 + r_6^2 \\
f_4 &= r_1^2 + r_2^2 + r_3^2 \\
f_5 &= r_1 r_4 + r_1 r_5 + r_3 r_5 + r_3 r_6 + r_2 r_6 + r_2 r_4 \\
f_6 &= r_4^3 + r_5^3 + r_6^3 \\
f_7 &= r_1^3 + r_2^3 + r_3^3 \\
f_8 &= r_4^2 r_1 + r_5^2 r_1 + r_5^2 r_3 + r_6^2 r_3 + r_6^2 r_2 + r_4^2 r_2 \\
f_9 &= r_1^2 r_6 + r_3^2 r_4 + r_2^2 r_5
\end{aligned} \tag{1}$$

In this work, the internuclear distances $r_i (i = 1, 2, \dots, 6)$ were displaced by reciprocal function ($1/r_i$) beforehand and the nine FIs were further transformed to $y_i = f_i^{1/m}$, where m is the degree of the corresponding FI, which can effectively accelerate the convergence in the fitting procedure.

To address the special symmetry of the off-diagonal block that is antisymmetric with the permutation of the two H atom, we follow the method of Guan by introducing the dot-cross product coordinate.⁸

$$Q_{NHHH}^{(3)} = \frac{(\mathbf{R}_N - \mathbf{R}_{H_1}) \cdot (\mathbf{R}_N - \mathbf{R}_{H_2}) \times (\mathbf{R}_N - \mathbf{R}_{H_3})}{r_{NH_1} r_{NH_2} r_{NH_3}} \tag{2}$$

The refined functional form for the three blocks are

$$\begin{aligned}
H_{11}^d &= NN_1(\text{FI}) \\
H_{12}^d &= Q_{NHHH}^{(3)} NN_2(\text{FI}) + [Q_{NHHH}^{(3)}]^3 NN_3(\text{FI}) \\
H_{22}^d &= NN_4(\text{FI})
\end{aligned} \tag{3}$$

where $NN_i(\text{FI}) (i = 1 - 4)$ are neural network functions with respect to FIs.

The NNs with M layers can be denoted as $R - S^1 - S^2 - \dots - S^M$. Suppose that there are Q

pairs of input/output for this feedforward NNs. Note $p_{r,q}$ as the r th element of the q th input, $w_{i,j}^m$ as the weight connecting the j th neuron of the $(m-1)$ th layer with the i th neuron of the m th layer and b_i^m as the bias of the i th neuron of the m th layer. Denote n_i^m and a_i^m as the net input and the output of the i th neuron of the m th layer, respectively. f^m represents the transfer function of the m th layer. For the q th input, n_i^m and a_i^m are denoted below by the superscript “ q ”. Then the NNs functions can be calculated by the formula:

$$n_{i,q}^m = \sum_{j=1}^{S^{m-1}} (w_{i,j}^m a_{j,q}^{m-1}) + b_i^m, a_{i,q}^m = f^m(n_{i,q}^m) \quad (4)$$

where $m = 1, 2, \dots, M$, $a_{i,q}^0 = p_{i,q}$, $S^0 = R$.

The gradient of NNs function with respect to its input can be obtained through the following equations:

$$\frac{\partial a_{i,q}^m}{\partial p_{r,q}} = \frac{\partial a_{i,q}^m}{\partial n_{i,q}^m} \frac{\partial n_{i,q}^m}{\partial p_{r,q}} \quad (5)$$

and

$$\frac{\partial n_{i,q}^m}{\partial p_{r,q}} = \sum_{j=1}^{S^{m-1}} w_{i,j}^m \frac{\partial a_{j,q}^{m-1}}{\partial p_{r,q}} \quad (6)$$

In the input layer (layer 0),

$$\frac{\partial a_{i,q}^0}{\partial p_{r,q}} = \delta_{i,r} \quad (7)$$

Starting in the input layer, then using Eqs.6 and 5, the gradient of NNs output with respect to the input, $\frac{\partial a_{k,q}^M}{\partial p_{r,q}}$, can be calculated. The closed analytical forms of the derivatives of the NNs output and its gradients with respect to NNs parameters can be obtained using the standard backpropagation algorithm.⁹

The accurate topography of diabatization

It is well known that close contour integration over *ab initio* calculated derivative couplings gives topological phase $n\pi$, if the contour encircles n number of CIs. Since the derivative couplings can be considered as the derivative of the *mixing angle* for two-state cases, the following condition

should be satisfied: If the contour encircles a conical intersection, the *mixing angle* accumulates a change of π .

For two-state cases, the real symmetric diabatic potential matrix can be represented with respect to the so-called *mixing angle* or *rotation angle*, λ :

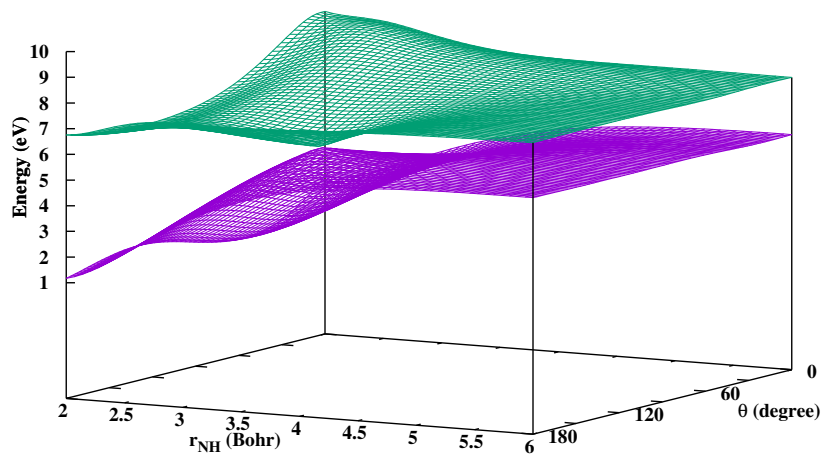
$$\begin{aligned} H_{11}^d &= E_1 \cos^2 \lambda + E_2 \sin^2 \lambda, \\ H_{12}^d &= (E_1 - E_2) \sin \lambda \cos \lambda, \\ H_{22}^d &= E_1 \sin^2 \lambda + E_2 \cos^2 \lambda. \end{aligned} \tag{8}$$

A conical intersection between ground and excited states can be observed in Fig. S1(a). By using $\lambda = \frac{1}{2} \arctan[-2 \frac{H_{12}^d}{H_{22}^d - H_{11}^d}]$ according to eq. (8), the *mixing angle* in the two-dimensional space is obtained as shown in the Fig. S1(b). We can see discontinuities in λ around the conical intersection. These discontinuities are not wrong but rather manifestations of the geometric phase effect (GPE), which can be examined by investigating the changes in *mixing angle* along closed paths. As can be seen, if a closed circular path circles the CI, the *mixing angle* accumulates a change of π , as shown in Fig. S1(b) and Fig. S2.

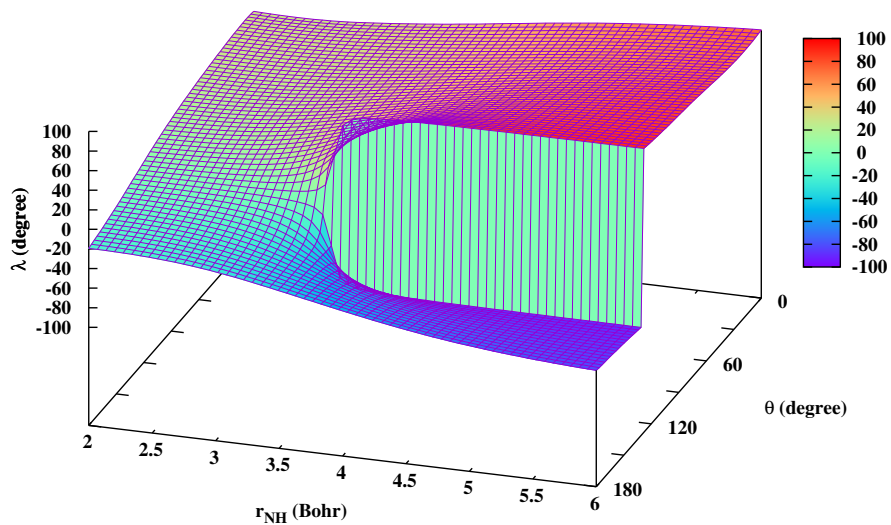
References

- (1) Evenhuis, C. R.; Collins, M. A. Interpolation of diabatic potential energy surfaces. *J. Chem. Phys.* **2004**, *121*, 2515–2527.
- (2) Godsi, O.; Evenhuis, C. R.; Collins, M. A. Interpolation of multidimensional diabatic potential energy matrices. *J. Chem. Phys.* **2006**, *125*, 104105.
- (3) Shu, Y.; Kryven, J.; Sampaio de Oliveira-Filho, A. G.; Zhang, L.; Song, G.-L.; Li, S. L.; Meana-Pañeda, R.; Fu, B.; Bowman, J. M.; Truhlar, D. G. Direct diabaticization and analytic representation of coupled potential energy surfaces and couplings for the reactive quenching of the excited $^2\Sigma^+$ state of OH by molecular hydrogen. *J. Chem. Phys.* **2019**, *151*, 104311.

- (4) Fu, B.; Kamarchik, E.; Bowman, J. M. Quasiclassical trajectory study of the postquenching dynamics of OH $A^2\Sigma^+$ by H₂/D₂ on a global potential energy surface. *J. Chem. Phys.* **2010**, *133*, 164306.
- (5) Zhu, X.; Yarkony, D. R. Toward eliminating the electronic structure bottleneck in nonadiabatic dynamics on the fly: An algorithm to fit nonlocal, quasidiabatic, coupled electronic state Hamiltonians based on ab initio electronic structure data. *J. Chem. Phys.* **2010**, *132*, 104101.
- (6) Shao, K.; Chen, J.; Zhao, Z.; Zhang, D. H. Communication: Fitting potential energy surfaces with fundamental invariant neural network. *J. Chem. Phys.* **2016**, *145*, 071101.
- (7) Chen, R.; Shao, K.; Fu, B.; Zhang, D. H. Fitting potential energy surfaces with fundamental invariant neural network. II. Generating fundamental invariants for molecular systems with up to ten atoms. *J. Chem. Phys.* **2020**, *152*, 204307.
- (8) Guan, Y.; Guo, H.; Yarkony, D. R. Neural network based quasi-diabatic Hamiltonians with symmetry adaptation and a correct description of conical intersections. *J. Chem. Phys.* **2019**, *150*, 214101.
- (9) Dennis Jr, J. E.; Schnabel, R. B. *Numerical methods for unconstrained optimization and nonlinear equations*; Siam, 1996; Vol. 16.



(a)



(b)

Figure S1: 3D plots of \mathbf{H}^d determined adiabatic energies (Panel a) and the *mixing angle* (Panel b) as a function of the dissociative N–H bond r_{NH} and the inversion angle θ . θ is the angle between the dissociative N–H bond and the C_3 axis and the other coordinates are fixed at the equilibrium geometry of the \tilde{X} state.

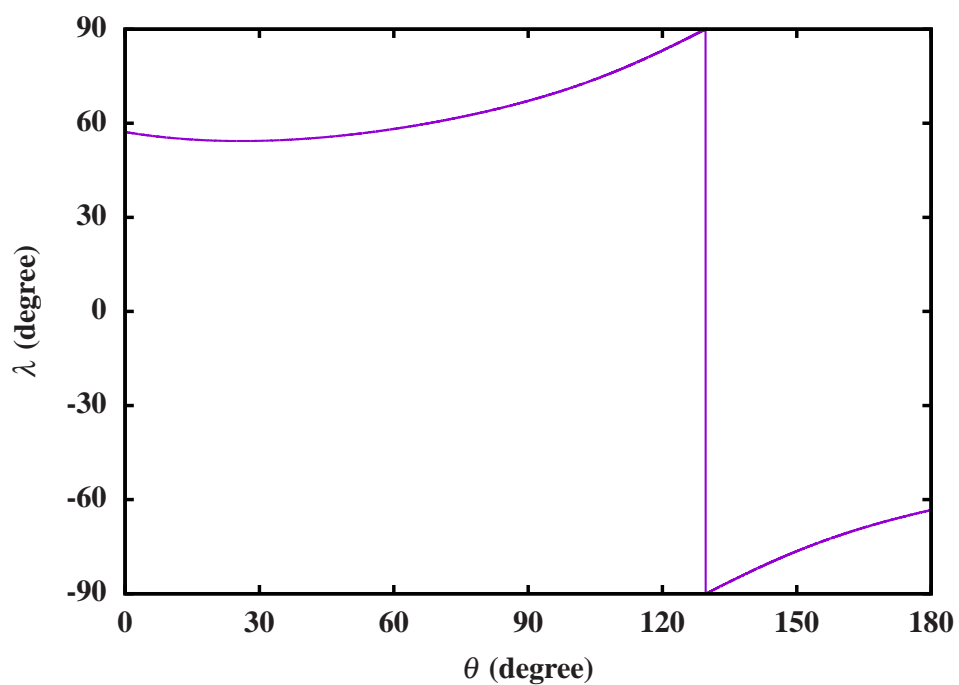


Figure S2: Plot of the *mixing angle* as a function of the inversion angle θ with the dissociative N–H bond $r_{\text{NH}} = 4.5$ bohr. θ is the angle between the dissociative N–H bond and the C_3 axis and the other coordinates are fixed at the equilibrium geometry of the \tilde{X} state.

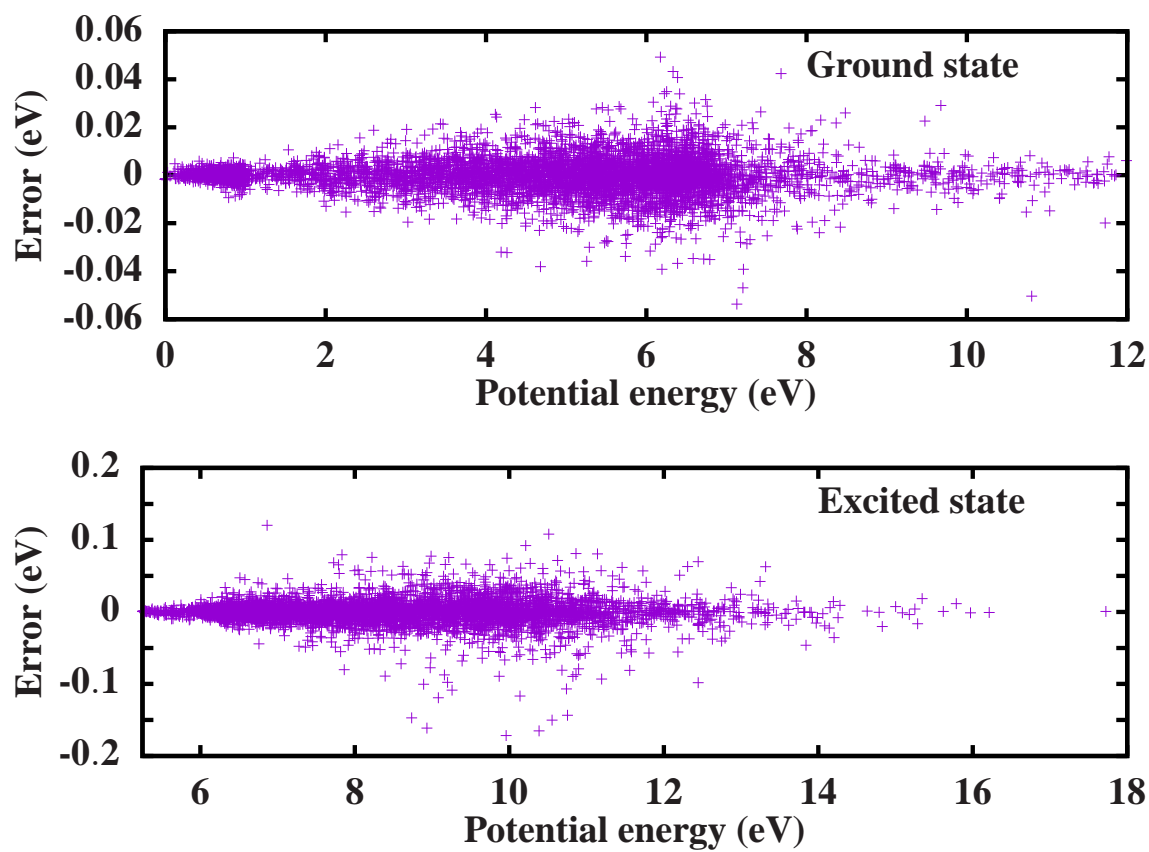


Figure S3: The distributions of fitting errors as a function of the adiabatic potential energy for the ground (a) and excited (b) states .

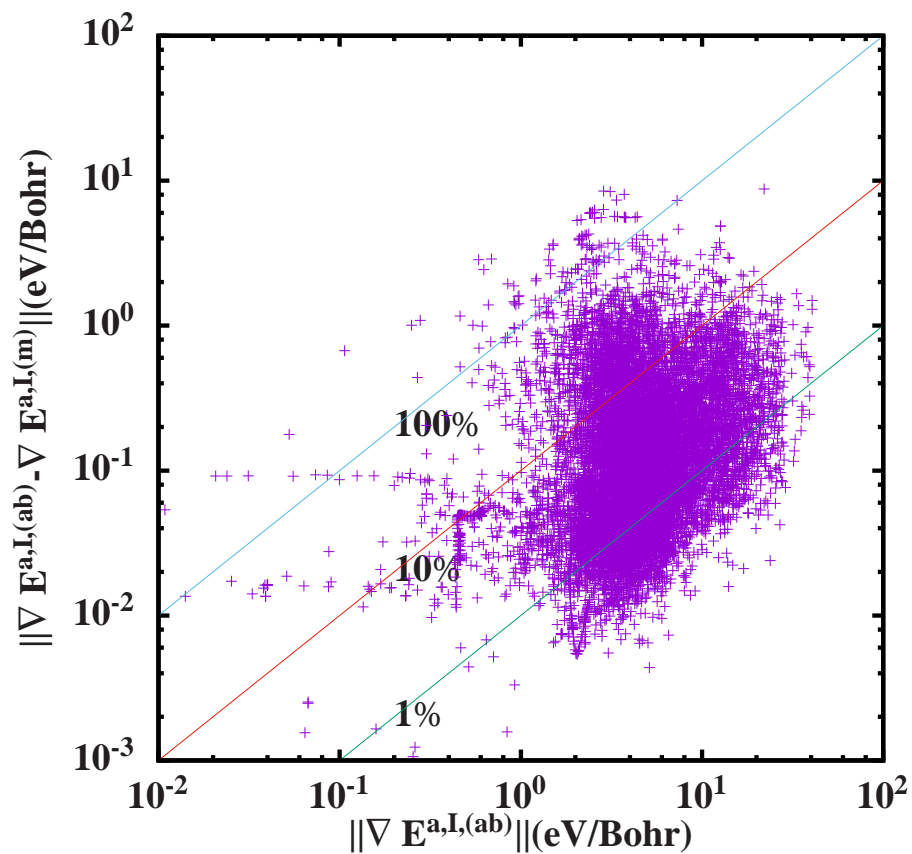
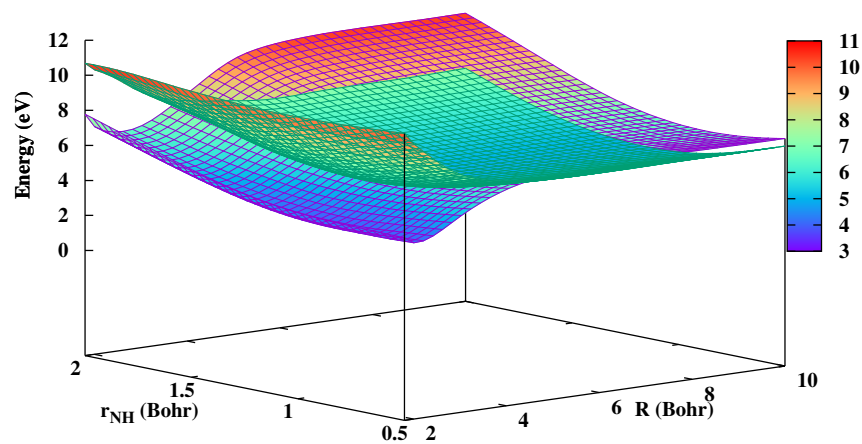
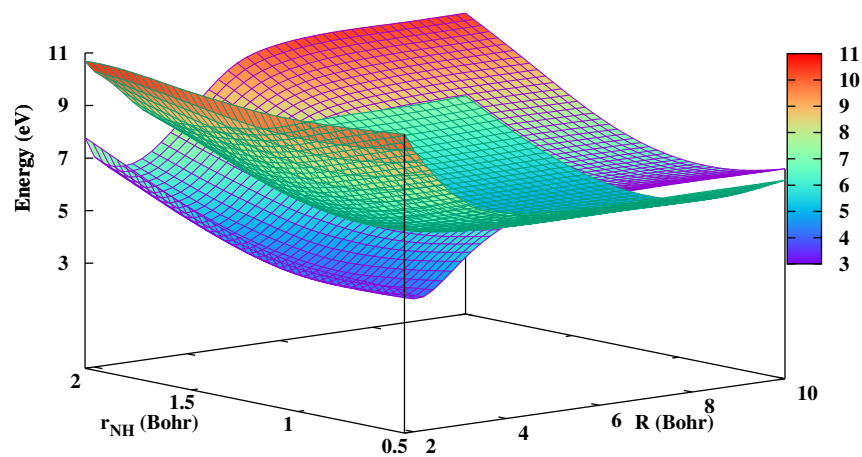


Figure S4: Comparison of the fitting error between \mathbf{H}^d determined energy gradients, $\|\nabla E^{a,I,(ab)} - \nabla E^{a,I,(m)}\|$, and *ab initio* energy gradients, $\|\nabla E^{a,I,(ab)}\|$ ($I = 1, 2$). The blue, red and green solid lines represent the 100%, 10% and 1% fitting error, respectively.



(a)



(b)

Figure S5: 3D plots of \mathbf{H}_{11}^d and \mathbf{H}_{22}^d as a function of r_{NH} and R for two different C_{2v} geometries. (a) The H–NH₂ C_{2v} geometries and (b) NH₂–H C_{2v} geometries with the H–H bond of the fragment NH₂ fixed at 3.2 Bohr, R being the distance between N and the center of mass of H₂ of the fragment NH₂ and r_{NH} being the distance of N and the dissociating H.